https://ntrs.nasa.gov/search.jsp?R=20090022184 2019-08-30T07:01:47+00:00Z

NASA/TM—2009-215501 AIAA–2008–5879

Reliability-Based Design Optimization of a Composite Airframe Component

Surya N. Patnaik
Ohio Aerospace Institute, Brook Park, Ohio

Shantaram S. Pai and Rula M. Coroneos
Glenn Research Center, Cleveland, Ohio

April 2009

NASA STI Program . . . in Profile

Since its founding, NASA has been dedicated to the advancement of aeronautics and space science. The NASA Scientific and Technical Information (STI) program plays a key part in helping NASA maintain this important role.

The NASA STI Program operates under the auspices of the Agency Chief Information Officer. It collects, organizes, provides for archiving, and disseminates NASA's STI. The NASA STI program provides access to the NASA Aeronautics and Space Database and its public interface, the NASA Technical Reports Server, thus providing one of the largest collections of aeronautical and space science STI in the world. Results are published in both non-NASA channels and by NASA in the NASA STI Report Series, which includes the following report types:

- TECHNICAL PUBLICATION. Reports of completed research or a major significant phase of research that present the results of NASA programs and include extensive data or theoretical analysis. Includes compilations of significant scientific and technical data and information deemed to be of continuing reference value. NASA counterpart of peer-reviewed formal professional papers but has less stringent limitations on manuscript length and extent of graphic presentations.

- TECHNICAL MEMORANDUM. Scientific and technical findings that are preliminary or of specialized interest, e.g., quick release reports, working papers, and bibliographies that contain minimal annotation. Does not contain extensive analysis.

- CONTRACTOR REPORT. Scientific and technical findings by NASA-sponsored contractors and grantees.

- CONFERENCE PUBLICATION. Collected papers from scientific and technical conferences, symposia, seminars, or other meetings sponsored or cosponsored by NASA.

- SPECIAL PUBLICATION. Scientific, technical, or historical information from NASA programs, projects, and missions, often concerned with subjects having substantial public interest.

- TECHNICAL TRANSLATION. English-language translations of foreign scientific and technical material pertinent to NASA's mission.

Specialized services also include creating custom thesauri, building customized databases, organizing and publishing research results.

For more information about the NASA STI program, see the following:

- Access the NASA STI program home page at *http://www.sti.nasa.gov*

- E-mail your question via the Internet to *help@sti.nasa.gov*

- Fax your question to the NASA STI Help Desk at 301–621–0134

- Telephone the NASA STI Help Desk at 301–621–0390

- Write to:
  NASA Center for AeroSpace Information (CASI)
  7115 Standard Drive
  Hanover, MD 21076–1320

NASA/TM—2009-215501 AIAA–2008–5879

Reliability-Based Design Optimization of a Composite Airframe Component

Surya N. Patnaik
Ohio Aerospace Institute, Brook Park, Ohio

Shantaram S. Pai and Rula M. Coroneos
Glenn Research Center, Cleveland, Ohio

Prepared for the
12th Multidisciplinary Analysis and Optimization Conference
sponsored by the American Institute of Aeronautics and Astronautics (AIAA) and the International Society for Structural and Multidisciplinary Optimization (ISSMO)
Victoria, British Columbia, Canada, September 10–12, 2008

National Aeronautics and
Space Administration

Glenn Research Center
Cleveland, Ohio 44135

April 2009

Acknowledgments

The authors acknowledge the Boeing Company for funding this project. Dr. Cliff Chen's technical assistance and encouragement for this project are greatly appreciated.

This report contains preliminary findings, subject to revision as analysis proceeds.

Level of Review: This material has been technically reviewed by technical management.

Available from

NASA Center for Aerospace Information
7115 Standard Drive
Hanover, MD 21076–1320

National Technical Information Service
5285 Port Royal Road
Springfield, VA 22161

Available electronically at http://gltrs.grc.nasa.gov

Reliability-Based Design Optimization of a Composite Airframe Component

Surya N. Patnaik
Ohio Aerospace Institute
Brook Park, Ohio 44142

Shantaram S. Pai and Rula M. Coroneos
National Aeronautics and Space Administration
Glenn Research Center
Cleveland, Ohio 44135

Summary

A stochastic design optimization (SDO) methodology has been developed to design components of an airframe structure that can be made of metallic and composite materials. The design is obtained as a function of the risk level, or reliability, *p*. The design method treats uncertainties in load, strength, and material properties as distribution functions, which are defined with mean values and standard deviations. A design constraint or a failure mode is specified as a function of reliability *p*. Solution to stochastic optimization yields the weight of a structure as a function of reliability *p*. Optimum weight versus reliability *p* traced out an inverted-S-shaped graph. The center of the inverted-S graph corresponded to 50 percent ($p = 0.5$) probability of success. A heavy design with weight approaching infinity could be produced for a near-zero rate of failure that corresponds to unity for reliability *p* (or $p = 1$). Weight can be reduced to a small value for the most failure-prone design with a reliability that approaches zero ($p = 0$). Reliability can be changed for different components of an airframe structure. For example, the landing gear can be designed for a very high reliability, whereas it can be reduced to a small extent for a raked wingtip. The SDO capability is obtained by combining three codes: (1) The MSC/Nastran code was the deterministic analysis tool, (2) The fast probabilistic integrator, or the FPI module of the NESSUS software, was the probabilistic calculator, and (3) NASA Glenn Research Center's optimization testbed CometBoards became the optimizer. The SDO capability requires a finite element structural model, a material model, a load model, and a design model. The stochastic optimization concept is illustrated considering an academic example and a real-life raked wingtip structure of the Boeing 767–400 extended range airliner made of metallic and composite materials.

Introduction

Engineers have recognized the existence of uncertainty in material properties, in load, and in structural analysis as well as in design constraints. Consider for example the yield strength of a steel that is required to design a steel structure. Strength is measured in the laboratory from tests conducted on standard coupons. It is commonly observed that repeated tests yield different values for the strength of steel. The test data can be processed to obtain a nominal or mean value and a dispersion range or a standard deviation. The nominal strength along with a safety factor is used to define allowable strength for traditional deterministic design calculations. Alternatively, strength can be considered as a random variable with a mean value and a standard deviation. The experimental data can be processed to obtain a probability distribution function such as, for example, the commonly used normal distribution function that is defined by a mean value and a standard deviation. This concept for strength can be extended to Young's modulus, Poisson's ratio, density, and so forth, and a probabilistic material model can be generated. The procedure can be repeated and a probabilistic load model can be developed for mechanical, thermal, and

initial deformation loads. Likewise, a probabilistic design model can be developed for sizing variables like depth and thickness of a beam.

Because of the stochastic nature of load, material properties, and sizing variables, structural response consisting of stress, strain, displacement, and frequency become random parameters with mean values and standard deviations. The cumulative distribution concept can be utilized to estimate the value of a response parameter for a specified level of probability. For example, the value of displacement in a particular structure at a location in a direction can be estimated to be less than 0.18 in. for a 25-percent probability of success or reliability. The value can change to less than 0.23 in. for 75 percent reliability. The concept illustrated for displacement can be extended to failure modes or design constraints, which become a function of reliability. In other words, a structure can be designed for a specified reliability between 0 and 1. High reliability can lead to a heavier design. The design is likely to be lighter when reliability is compromised. In other words, the weight of a structure becomes a function of the reliability. It would be shown that reliability versus weight traced out an inverted-S-shaped graph.

Reliability-based design optimization requires a probabilistic analysis tool. Several such tools are discussed in References 1 and 2. Here, the Fast Probabilistic Integrator (FPI) module of the NESSUS code (Ref. 3) is used for probabilistic calculation for the industrial strength wingtip problem. A quadratic perturbation method (Ref. 1) is used for the academic problems. The probabilistic response is used to formulate the stochastic design problem. It is solved using an optimization testbed, which in the literature is referred to as CometBoards (Ref. 4). The probabilistic analysis and design concepts are illustrated for an academic example and for an industrial strength aircraft wingtip structure made of metallic and composite materials. The subject matter of the paper is presented as follows: Probabilistic analysis is covered in the following section, then design optimization is discussed, and conclusions are presented at the end.

Probabilistic Structural Analysis

Popular probabilistic analysis formulations include Monte Carlo simulation, sampling and stratified sampling techniques, the Latin hypercube technique, response surface method, and others. Monte Carlo simulation (Ref. 5) is a powerful numerical approach, but it is repetitive and computationally expensive. Numerical integration, second-moment analysis, and stochastic finite element methods (Ref. 6) are also available. The perturbation method has been used extensively in developing the stochastic finite element method because of its simplicity, efficiency, and versatility. Cambou (Ref. 7) proposed a first-order perturbation method for the finite element solution of linear static problems. Cornell (Ref. 8) introduced a second-moment concept. During the 1980s, the method was developed further by Hisada and Nakagori (Ref. 9) for static and eigenvalue problems. The perturbation method was also adopted by Handa and Anderson (Ref. 10) for static problems of beam and frame structures. Applications of perturbation methods have also been reported by Benaroya (Ref. 11), Elishakoff (Ref. 12), and Schuëller (Ref. 13). In this paper, for academic problems a quadratic perturbation technique is employed to calculate the mean value and the covariance matrix in closed form for stress and displacement. For the wingtip industrial problem, fast probability integration (FPI) is used, which is based on a most probable point (MPP) concept. The majority of the probability is concentrated near the MPP. The MPP is located and different probabilistic methods are used to determine the probability in the failure prone region. The probabilistic response is generated from a few deterministic solutions.

Perturbation Method

The perturbation method for probabilistic analysis has been developed for both force and displacement methods. The method of force used is referred to as the integrated force method (IFM) (Ref. 14). The dual of the primal IFM, or the dual integrated force method (IFMD) (Ref. 15), became the displacement method. The perturbation technique yields the mean value, and the covariance matrix for the response variables like internal force and displacement. The cumulative distribution concept is applied to

determine the response for a specified distribution function and a probability level. The parameters for perturbation, or the primitive random variables, are separated into three groups. These are loads, material properties, and design variables. The load vector encompasses mechanical load, thermal load, and settling of support or initial deformation load. It is defined in terms of a mean load vector and a covariance matrix. Material properties considered are elastic modulus, Poisson's ratio, coefficient of thermal expansion, and density. Their mean values and the associated covariance matrices are the stochastic parameters. The sizing design parameters are the areas of bars, moment of inertia of beams, thickness of plates, and so forth. Their stochastic parameters are defined through mean values and a covariance matrix. The geometrical parameters like length of a truss bar and spans of a plate are considered as deterministic variables.

Quadratic Perturbation Technique

In the perturbation technique, the mean value and the covariance matrix of a response variable are obtained in two basic steps. First, a response variable is expanded in a Taylor's series with respect to the primitive random variables. The linear and quadratic terms are retained in the series expansion. An application of the expectation operator E[..] yielded the expressions for mean value and the covariance matrix.

Prior to the expansion, the primitive parameters are scaled to obtain a normalized variable (q) with a zero mean and a small variance. Consider, for example, the coefficient of thermal expansion α with a mean μ_α and a standard deviation σ_α. Its normalized variable q_α is defined as

$$q_\alpha = \frac{\alpha - \mu_\alpha}{\mu_\alpha} \tag{1a}$$

or

$$\alpha = \mu_\alpha \left(1 + q_\alpha\right) \tag{1b}$$

The mean value of q_α is obtained by using the expectation operator (E[..]):

$$\mu_{q_\alpha} = \mathrm{E}\left[\frac{\alpha - \mu_\alpha}{\mu_\alpha}\right] = \frac{\mathrm{E}[\alpha] - \mathrm{E}[\mu_\alpha]}{\mu_\alpha} = \frac{\mu_\alpha - \mu_\alpha}{\mu_\alpha} = 0 \tag{2a}$$

The variance of q_α is obtained as

$$\begin{aligned} \sigma^2_{q_\alpha} &= \mathrm{E}\left[\left(q_\alpha - \mu_{q_\alpha}\right)^2\right] \\ &= \mathrm{E}\left[\left(\frac{\alpha - \mu_\alpha}{\mu_\alpha} - 0\right)^2\right] \\ &= \left(\frac{1}{\mu^2_\alpha}\right)\mathrm{E}\left[\left(\alpha - \mu_\alpha\right)^2\right] \\ &\equiv \frac{\sigma^2_\alpha}{\mu^2_\alpha} \end{aligned} \tag{2b}$$

The variance of α is assumed to be much smaller than the square of its mean. This justifies the use of a Taylor expansion of response variables in terms of the normalized primitive random variables. The Taylor series expansion is discussed considering the example of the internal force vector $\{F\}$. The expansion can be expressed as

$$\{F\} = \{\bar{F}\} + \left(\{q\}^T \overline{\mathcal{L}\{F\}}\right) + \frac{1}{2}\left(\{q\}^T \overline{\mathcal{L}\{F\}\mathcal{L}^T}\{q\}\right) + \text{higher order term} \tag{3}$$

where

$$\left(\{q\}^T \overline{\mathcal{L}(\bullet)}\right) = \sum_i q_i \left.\frac{\partial(\bullet)}{\partial q_i}\right|_{\{q\}=\{0\}}$$

and

$$\left(\{q\}^T \overline{\mathcal{L}(\bullet)\mathcal{L}^T}\{q\}\right) = \sum_{i,j} q_i q_j \left.\frac{\partial^2(\bullet)}{\partial q_i \partial q_j}\right|_{\{q\}=\{0\}}$$

Similar expansions are also obtained for the governing matrix $[S]$ of IFM, the load vector $\{P\}$, displacement $\{X\}$, the flexibility matrix $[G]$, and initial deformation $\{\tilde{\beta}\}$, where their deterministic (or over-bar) quantities are calculated by setting the normalized primitive random variables to zero ($q_i = 0$). Four steps are followed to derive the expressions for the mean value and the covariance matrix of the force vector:

Step 1. Substitute the Taylor series expansions into the IFM governing equation, see References 1 and 2. The left-hand side contains a single zero-order term, two linear terms, and three quadratic terms in the normalized primitive random variables, and the right-hand side has one term of each order.

Step 2. Equate equal order terms. The zero-order term gives the deterministic solution. The linear terms drop out. The second-order terms produce an equation with four quadratic terms on the right-hand side and a single term on the left-hand side.

Step 3. Take the expectation E[..] of terms in Step 2 to obtain the mean value of the force vector.

Step 4. Take the expectation E[..] of the product $\{F\}\{F\}^T$, and subtract the square of the mean of the force vector, as calculated in Step 3, to obtain the covariance matrix of the force vector.

The expressions for mean value and covariance matrix for force and displacement vectors via IFM, listed in Reference 1, is not repeated here. The process was repeated next for the IFMD to obtain similar expressions, also listed in Reference 1. The derivation included mechanical and initial deformation loads. The mean value of the force and displacement contained zero-order and quadratic terms, but not linear terms, in the Taylor series. However, the covariance matrix retained the zero-order, linear, and quadratic terms of expansions. For simple academic structures the expressions were programmed in closed form in Macsyma software (Ref. 16).

Illustrative Example: Three-Bar Truss

Stochastic response analysis is illustrated considering the example of a three-bar truss shown in Figure 1. The geometrical dimensions of the structure like the coordinates of the four nodes and bar lengths are considered deterministic in nature. The structure has a total of 10 primitive random variables for the material properties, load, and sizing design parameters.

Material Model: The truss is made of steel, and it has two random material variables: the Young's modulus and the coefficient of thermal expansion. The Young's modulus E has a mean value of $\mu_E = 30\,000$ ksi and standard deviation of 3000 ksi. The coefficient of thermal expansion α has a mean value of $\mu_\alpha = 6.6\times10^{-6}$/°F and standard deviation of 6.6×10^{-7}/°F.

Mechanical Load Model: The structure is subjected to mechanical and thermal loads as well as loads due to settling of support. Mechanical load is defined by its mean value and covariance matrix. The load $\begin{Bmatrix} P_X \\ P_Y \end{Bmatrix}$ is applied at the free node 1.

Mean value: $\begin{Bmatrix} \mu_{P_X} \\ \mu_{P_Y} \end{Bmatrix} = \begin{Bmatrix} 50 \\ -100 \end{Bmatrix}$ kip

Covariance matrix: $\mathrm{cov}\left(\begin{Bmatrix} P_X \\ P_Y \end{Bmatrix}\right) = \begin{bmatrix} 25.00 & 6.25 \\ 6.25 & 25.00 \end{bmatrix}$

Thermal Load Model: Node 1 of the structure is subjected to a change of temperature, with a mean of $\mu_T = 50$ °F and a standard deviation of 5 °F. The other three nodes are at ambient temperature. Thermal load is obtained for the bar temperature, which is calculated from the average of the temperatures at its two connecting nodes.

Load Due to Settling of Support: Support node 2 settles in both the x- and y-directions by amount $\begin{Bmatrix} \Delta_{2X} \\ \Delta_{2Y} \end{Bmatrix}$ inches as shown in Figure 1. Settling is accommodated by a mean value and a covariance matrix.

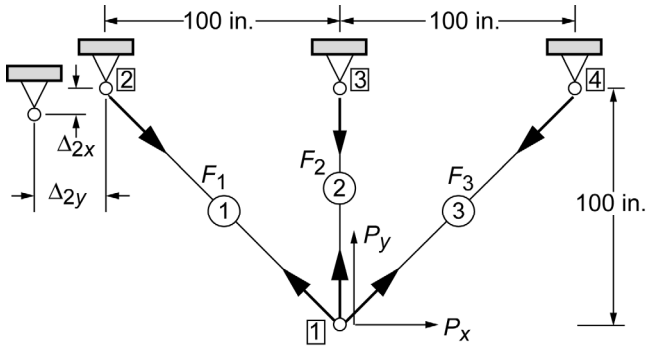

Figure 1.—Three-bar truss, where P is load, F is force, and Δ is setting of support.

Mean value: $\left\{\begin{matrix}\mu_{\Delta_{2X}}\\ \mu_{\Delta_{2Y}}\end{matrix}\right\}=\left\{\begin{matrix}0.1\\ 0.15\end{matrix}\right\}$ in.

Covariance matrix: $\operatorname{cov}\left(\left\{\begin{matrix}\Delta_{2X}\\ \Delta_{2Y}\end{matrix}\right\}\right)=\begin{bmatrix}25.0 & 37.5\\ 37.5 & 225.0\end{bmatrix}\times 10^{-6}$

Design Model: The areas of the three bars (A_1, A_2, and A_3) are considered to be the design variables. Their mean value and covariance matrix are as follows:

Mean value: $\left\{\begin{matrix}\mu_{A_1}\\ \mu_{A_2}\\ \mu_{A_3}\end{matrix}\right\}=\left\{\begin{matrix}1\\ 1\\ 2\end{matrix}\right\}$ in.^{2}

Covariance matrix: $\operatorname{cov}\left(\left\{\begin{matrix}A_1\\ A_2\\ A_3\end{matrix}\right\}\right)=\begin{bmatrix}1.00 & 0.50 & 0.25\\ 0.50 & 1.00 & 0.25\\ 0.25 & 0.25 & 1.00\end{bmatrix}\times 10^{-2}$

The 10 random variables of the problem are scaled to obtain the 10 primitive variables q_1, q_2,…,q_{10}, which are defined as

$$\begin{aligned}
A_1 &= \mu_{A_1}\left(1+q_{A_1}\right) &&= \mu_1\left(1+q_1\right)\\
A_2 &= \mu_{A_2}\left(1+q_{A_2}\right) &&= \mu_2\left(1+q_2\right)\\
A_3 &= \mu_{A_3}\left(1+q_{A_3}\right) &&= \mu_3\left(1+q_3\right)\\
E &= \mu_E\left(1+q_E\right) &&= \mu_4\left(1+q_4\right)\\
\alpha &= \mu_\alpha\left(1+q_\alpha\right) &&= \mu_5\left(1+q_5\right)\\
P_X &= \mu_{P_X}\left(1+q_{P_X}\right) &&= \mu_6\left(1+q_6\right)\\
P_Y &= \mu_{P_Y}\left(1+q_{P_Y}\right) &&= \mu_7\left(1+q_7\right)\\
T &= \mu_T\left(1+q_T\right) &&= \mu_8\left(1+q_8\right)\\
\Delta_1 &= \mu_{\Delta_1}\left(1+q_{\Delta_1}\right) &&= \mu_9\left(1+q_9\right)\\
\Delta_2 &= \mu_{\Delta_2}\left(1+q_{\Delta_2}\right) &&= \mu_{10}\left(1+q_{10}\right)
\end{aligned} \tag{4}$$

The normalized primitive random variable, $\{q\}$, with zero mean, and standard deviation given by the ratio of the standard deviation to the mean of the corresponding stochastic variable is assumed to be of order o(1). This justifies the use of a Taylor series expansion in $\{q\}$. Only up to quadratic terms are retained in the series.

The deterministic response for forces and displacements are as follows:

Bar forces: $\{F\} = \{\mu_F\} = \begin{Bmatrix} 62.76 \\ 61.24 \\ -7.95 \end{Bmatrix}$ kip

Nodal displacements: $\{X\} = \{\mu_X\} = \begin{Bmatrix} 0.201 \\ -0.241 \end{Bmatrix}$ in.

The probabilistic response for bar forces consists of the mean values and the covariance matrix as follows:

Mean values of bar forces: $\{\mu_{\bar{F}}\} = \begin{Bmatrix} 62.78 \\ 61.22 \\ -7.93 \end{Bmatrix}$ kip

Covariance matrix of forces: $\text{cov}(F) = \begin{bmatrix} 19.27 & 1.78 & -4.48 \\ 1.78 & 18.93 & -8.83 \\ -4.48 & -8.83 & 21.78 \end{bmatrix}$

Correlation matrix for forces: $\left[\frac{\rho_{ij}^{\ 2}}{(\rho_i)(\rho_j)}\right] = \rho_F = \begin{bmatrix} 1.0 & 0.093 & -0.219 \\ 0.093 & 1.0 & -0.435 \\ -0.219 & -0.435 & 1.0 \end{bmatrix}$

Likewise, the probabilistic response for nodal displacements are

Mean values of displacements: $\{\mu_{\bar{X}}\} = \begin{Bmatrix} 0.197 \\ -0.237 \end{Bmatrix}$ in.

Covariance matrix of displacements: $\text{cov}(X) = \begin{bmatrix} 12.2 & -8.9 \\ -8.9 & 8.7 \end{bmatrix} \times 10^{-4}$

Correlation matrix for displacements: $\rho_X = \begin{bmatrix} 1.0 & -0.866 \\ -0.866 & 1.0 \end{bmatrix}$

where the elements of ρ_F and ρ_X are the correlation coefficients.

For the bar forces, there is very little difference between the mean value $\{\mu_{\bar{F}}\}$ and the deterministic solution $\{\mu_F\}$. For the nodal displacements also, there was little difference between the mean value $\{\mu_{\bar{X}}\}$ and the deterministic solution $\{\mu_X\}$. For all examples, big or small, it was observed that the mean value was quite close to the deterministic solution, which however, has not been proved analytically.

The standard deviations for the bar forces were about 7 percent for bars 1 and 2. However, it was 59 percent for the bar 3. The variation in the primitive variables like mechanical, thermal, and settling of support loads was between 5 and 10 percent. The variation in the response or bar forces of the basic structure is comparable to that for the load variation. However, the variation in the redundant bar force at 59 percent is 6 times that of the load.

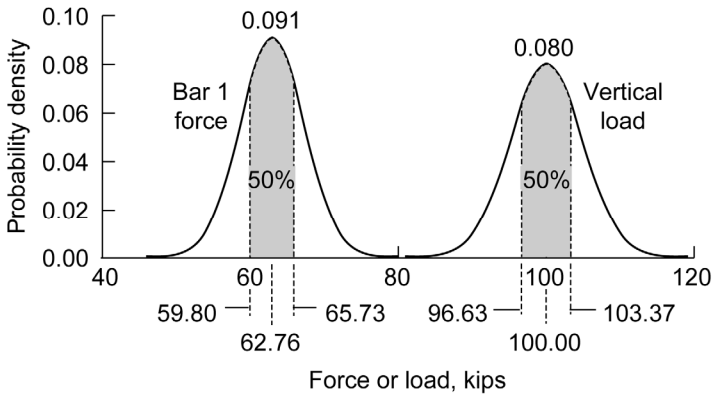

Figure 2.—Probability density function for bar 1 force and vertical load.

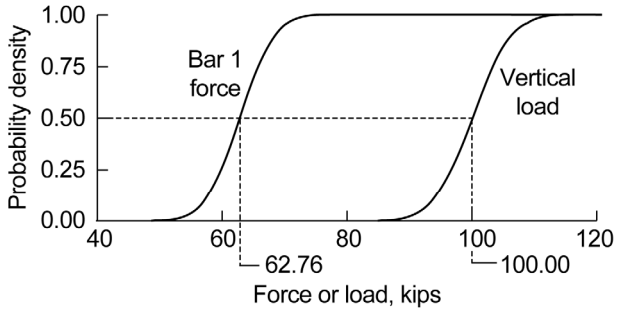

Figure 3.—Cumulative distribution function for bar 1 force and vertical load.

The standard deviations for the displacements are between 12 and 17 percent, which are higher than the load variation. The variations for the displacements are more pronounced than that for the bar forces because these are susceptible to loads as well as to material properties and design variables.

The probability density function and the cumulative distribution function for the bar 1 force and magnitude of the vertical load are depicted in Figures 2 and 3, respectively. There is 50-percent likelihood that the first bar force (with a mean of 62.67 kips) is between 59.80 and 65.73 kips.

The value of the response variables for percent probability of success p = 50, 25, and 75 percent are listed in Table I. A 5-percent change was seen in the forces of bars 1 and 2 between the p = 50 percent and p = 75 percent levels. For the bar 3 force, the change noted was 40 percent. A 12-percent change was seen in the horizontal displacement between the p = 50 percent and p = 75 percent levels. It was only 8 percent for the vertical displacement.

TABLE I.—STOCHASTIC RESPONSE FOR THREE-BAR TRUSS

Response variable	Upper limit of response variable (range) for probability of occurrence, p		
	50 percent (mean)	25 percent	75 percent
Bar force, kips			
F_1	62.76	59.80 (95%)	65.73 (105%)
F_2	61.24	58.30 (95%)	64.17 (105%)
F_3	–7.95	–4.80 (60%)	–11.09 (140%)
Displacement, in.			
u	0.201	0.178 (88%)	0.225 (112%)
v	–0.241	–0.221 (92%)	–0.261 (108%)

The sensitivity of the bar 1 force and the vertical displacement at the 75-percent probability of occurrence level with respect to the 10 primitive random variables are shown in Figures 4 and 5, respectively. The maximum value along the y-axis in Figures 4 and 5 are normalized to unity. The bar force is equally sensitive to the areas of bars 1 and 2 in magnitude, but opposite in directions. The sensitivity of the bar 1 force with respect to the bar 3 area is very small. The vertical displacement is equally sensitive to the areas of bars 1 and 2, but is insensitive to the bar 3 area. The Young's modulus has little effect on the bar force but has the most effect of all the primitive variables on the vertical displacement. The sensitivities with respect to thermal coefficient and temperature are identical because the analysis uses their product as a single entity. Both load components strongly effect the bar force, whereas only the vertical load effects the vertical displacement to the same degree. Temperature and settling of support loads have a moderate effect.

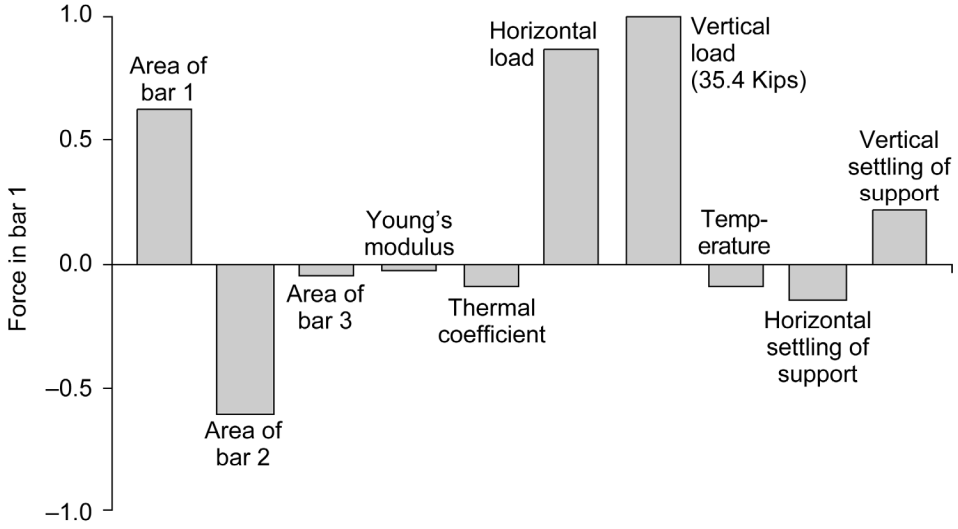

Figure 4.—Sensitivities for bar 1 force at 75 percent probability level with respect to 10 random variables.

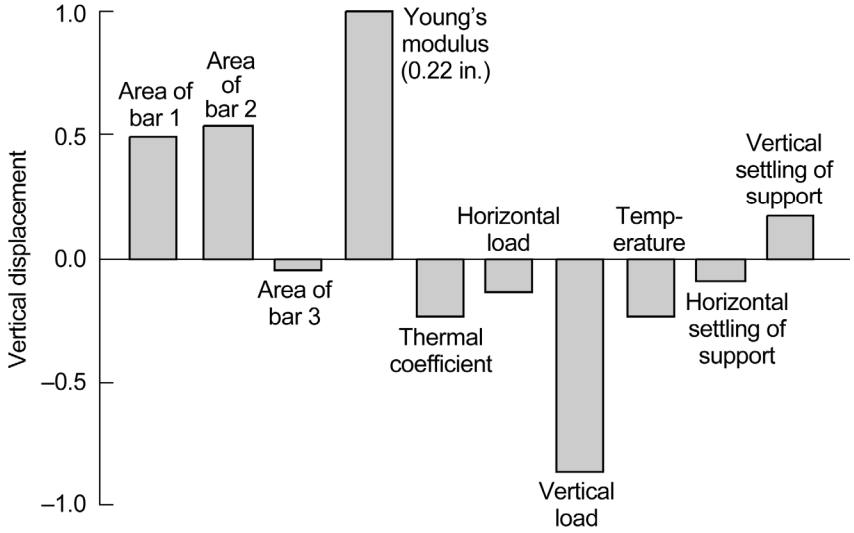

Figure 5.—Sensitivities for vertical displacement at 75 percent probability level with respect to 10 random variables.

Comparison With Other Methods

Stochastic response via perturbation method was compared with other probabilistic formulations considering the example of the three-bar truss shown in Figure 1 with the same 10 random variables for the material properties, load, and sizing design parameters. A summary of response calculated by the four methods is depicted in Table II. Two different computers were used in the calculations shown in Table II. A Dell Inspiron desktop with four central processing units (CPUs) and 3.2 GHz processor was used to obtain most of the results. The FPI code shown in the last column was run in a very fast Red Hat Linux dual CPU workstation with a 32 GHz processor. The four methods compared were

(1) Perturbation method (PM)
(2) Direct Monte Carlo simulation (DMCS)
(3) Latin hypercube simulation (LHS)
(4) Fast probabilistic integration of the NESSUS code (FPI)

TABLE II.—PROBABILISTIC RESPONSE COMPARED FOR THREE-BAR TRUSS

Parameter	Perturbation method (PM)		Direct Monte Carlo simulation (DMCS)		Latin hypercube simulation (LHS)		Fast probability integrator (FPI)	
	Mean value	Standard deviation	Mean value	Standard deviation	Mean value	Standard deviation	Mean value	Standard deviation
Force: $\begin{Bmatrix}F_1\\F_2\\F_3\end{Bmatrix}^{\text{kip}}$	$\begin{Bmatrix}62.77\\61.24\\-7.95\end{Bmatrix}$	$\begin{Bmatrix}4.39\\4.35\\4.67\end{Bmatrix}$	$\begin{Bmatrix}62.77\\61.27\\-7.93\end{Bmatrix}$	$\begin{Bmatrix}4.39\\4.35\\4.67\end{Bmatrix}$	$\begin{Bmatrix}62.76\\61.25\\-7.96\end{Bmatrix}$	$\begin{Bmatrix}4.39\\4.35\\4.67\end{Bmatrix}$	$\begin{Bmatrix}62.78\\61.21\\-7.93\end{Bmatrix}$	$\begin{Bmatrix}4.39\\4.35\\4.67\end{Bmatrix}$
Stress: $\begin{Bmatrix}\sigma_1\\\sigma_2\\\sigma_3\end{Bmatrix}^{\text{ksi}}$	$\begin{Bmatrix}63.29\\61.70\\-3.98\end{Bmatrix}$	$\begin{Bmatrix}6.71\\6.20\\2.34\end{Bmatrix}$	$\begin{Bmatrix}63.16\\61.58\\-3.97\end{Bmatrix}$	$\begin{Bmatrix}5.89\\5.42\\2.79\end{Bmatrix}$	$\begin{Bmatrix}63.15\\61.57\\-3.99\end{Bmatrix}$	$\begin{Bmatrix}5.77\\5.38\\2.75\end{Bmatrix}$	$\begin{Bmatrix}62.78\\61.21\\-3.96\end{Bmatrix}$	$\begin{Bmatrix}6.34\\6.03\\2.69\end{Bmatrix}$
Displacement: $\begin{Bmatrix}u\\v\end{Bmatrix}^{\text{in.}}$	$\begin{Bmatrix}0.20\\-0.24\end{Bmatrix}$	$\begin{Bmatrix}0.004\\0.003\end{Bmatrix}$	$\begin{Bmatrix}0.20\\-0.24\end{Bmatrix}$	$\begin{Bmatrix}0.004\\0.003\end{Bmatrix}$	$\begin{Bmatrix}0.20\\-0.24\end{Bmatrix}$	$\begin{Bmatrix}0.004\\0.003\end{Bmatrix}$	$\begin{Bmatrix}0.20\\-0.24\end{Bmatrix}$	$\begin{Bmatrix}0.004\\0.003\end{Bmatrix}$
Computation time								
CPU seconds	7.0		4245		390			1
Normalized time	1.0		606		56			---

The stiffness method as implemented in the ANSYS code (Ref. 17) was used in the DMCS and in the LHS. Response was calculated via the primal and the dual integrated force methods (IFM and IFMD, respectively) in the perturbation and fast probability integration techniques. Both IFM and IFMD yield identical solutions for deterministic as well as stochastic calculations even though the structure of equations differed, at least in appearance (Ref. 1). Response for the three bar forces, stresses, and displacements by the four methods (PM, DCMS, LHS, and FPI) and time to solution (CPU seconds) are depicted in Table II. For bar forces, the mean values and standard deviations were in good agreement for all four methods. The displacements showed an almost perfect match across the four methods. There was a minor mismatch among the methods for bar stress. The maximum difference was about 0.8 percent in the mean value of the stress, whereas it was about 19 percent for standard deviation for the redundant member. Direct Monte Carlo simulation required 12 500 samples for convergence, whereas 1000 samples were sufficient for the Latin hypercube simulation. The time to calculate the response was very small, between 1 to 7 CPU seconds by the perturbation method as well as by the fast probability integrator. The calculation time increased many times for the Monte Carlo and Latin hypercube simulations. Monte Carlo simulation required about 4245 s, which corresponded to 606 times that required by the perturbation method. Latin hypercube method took 56 times as long. Overall, the performance was satisfactory for all

four methods. The Ph.D. dissertation of Wei (Ref. 2) provides merits and limitations of different probabilistic solution methods.

Probabilistic Design Optimization

Probabilistic design optimization accounts for the uncertainties in the model, like those in design variables, in loads, in strength, and in material properties. The design is obtained as a function of the risk level, or reliability, p. A design with a 50-percent rate of success (corresponding to one failure in two samples, or $N = 2$ and $p = 0.5$) is the mean-valued design. For the most reliable design the parameter p can approach unity. For example, for one failure in 50 000 samples, $p = 1 - 1/N = 0.99998$. For a design that is not reliable or prone to failure, p can approach 0, (e.g., for 999 failures in 1000 samples, $p = 0.001$). The constraints that represent failure modes are defined for a specified rate of failure.

A probabilistic design optimization problem can be formulated with two merit functions:

(1) Minimize the mean value of the weight
(2) Minimize the variation or the standard deviation of the weight

Consider for example, the three-bar truss shown in Figure 1. The area or diameter of a bar becomes the design variable. Probabilistic calculation can consider the determination of mean value and a standard deviation in the diameter. However, the standard deviation in the diameter is a manufacturing issue. A design process uses available members with specified diameter or cross-sectional areas.

Probabilistic optimization can be separated into reliability-based design and robust design. Reliability-based design minimizes the mean value of the objective function. Robust design simultaneously minimizes the mean value as well as the standard deviation of the objective function. This paper emphasizes reliability-based optimization. However, for completeness, the robust design concept is discussed for the three-bar truss shown in Figure 1.

The mean value and standard deviations of the objective function (f) can be defined as

$$\text{Mean value: } \mu_f = \mathrm{E}\left[\mathrm{f}(x)\right] = \iint \ldots \int \mathrm{f}(x)\,\mathrm{p}(x_1, x_2, \ldots x_k)\,\mathrm{d}x_1 \mathrm{d}x_2 \ldots \mathrm{d}x_k \tag{5a}$$

$$\text{Standard deviation: } \sigma_f = \mathrm{E}\left[\left(\mathrm{f}(x) - \mu_f\right)^2\right] = \iint \ldots \int \left(\mathrm{f}(x) - \mu_f\right)^2 \mathrm{p}(x_1, x_2, \ldots x_k)\,\mathrm{d}x_1 \mathrm{d}x_2 \ldots \mathrm{d}x_k \tag{5b}$$

where

$\mathrm{p}(x_1, x_2, \ldots x_k)$ is the joint probability density function
$\mathrm{f}(x)$ is the merit (or weight) function
x_i are the design variables
E[..] is the expectation operator

It is difficult to define the joint probability density function for an industrial-strength structural design problem. Here, normal distribution is assumed for the random variables, which are further considered to be independent. The robust design optimization problem can be reformulated as follows:

Minimize both mean value μ_f and standard deviation σ_f $\tilde{f} = \left[\mu_f, \sigma_f\right]$ for constraints

$\mathrm{E}\left[g_i(x)\right] + \beta_i \sigma\left(g_i(x)\right) \le 0$ within prescribed lower and upper bounds $x_L \le x \le x_U$

where

$\tilde{f}$ is a vector of two objective functions

μ_f is the mean value

σ_f is the standard deviation

β_i is a constraints (g_i) satisfactory index

Pareto optimality criteria (Ref. 18) is a classical technique to solve a multiobjective problem. Because of difficulty, however, the problem is transformed to a single composite objective function and solved. A composite objective is obtained by a linear combination of mean value and standard deviation with a weighting factor α in the range $0 \le \alpha \le 1$. The function of merit F can be written as

$$F = (1-\alpha)\frac{\mu_W}{\mu_W^*} + \alpha\frac{\sigma_W}{\sigma_W^*} \tag{6}$$

where μ_W^* and σ_W^* are the mean and standard deviation of weight, respectively, when solved independently.

The robust design of the three-bar truss shown in Figure 1 uses the data given for its analysis, along with a weight density that has a mean value of 0.289 lbf/in.^{3} with a standard deviation of 0.005 lbf/in.^{3}. The mean value and the standard deviation for the strength are 20 and 2 ksi, respectively. The optimum solution is given in Table III for different values of the parameter α for a 50-percent probability ($p = 0.5$). Mean value and standard deviation versus the parameter α are plotted in Figure 6 with an exaggerated scale along the y-axis.

TABLE III.—ROBUST DESIGN FOR THE THREE-BAR TRUSS

Design parameters	Weight factor, α				
	0	0.25	0.50	0.75	1.00
Area, in.^{2}: $\begin{Bmatrix} A_1 \\ A_2 \\ A_3 \end{Bmatrix}$	$\begin{Bmatrix} 1.1042 \\ 0.7359 \\ 0.1000 \end{Bmatrix}$	$\begin{Bmatrix} 1.1042 \\ 0.7359 \\ 0.1000 \end{Bmatrix}$	$\begin{Bmatrix} 1.1042 \\ 0.7360 \\ 0.100 \end{Bmatrix}$	$\begin{Bmatrix} 1.1042 \\ 0.7360 \\ 0.1000 \end{Bmatrix}$	$\begin{Bmatrix} 1.1042 \\ 0.7361 \\ 0.1000 \end{Bmatrix}$
Weight, lbf: $\begin{Bmatrix} \text{mean} \\ \text{variance} \end{Bmatrix}$	$\begin{Bmatrix} 70.4908 \\ 8.4504 \end{Bmatrix}$	$\begin{Bmatrix} 70.4889 \\ 8.4502 \end{Bmatrix}$	$\begin{Bmatrix} 70.4870 \\ 8.4500 \end{Bmatrix}$	$\begin{Bmatrix} 70.4863 \\ 8.4499 \end{Bmatrix}$	$\begin{Bmatrix} 70.4870 \\ 8.4500 \end{Bmatrix}$

The mean value and standard deviation versus the parameter α traced out the typical graph as shown in Figure 6. The robust design corresponding to the intersection point MS represents a simultaneous minimum for the mean value of weight as well as its standard deviation. The intersection occurred for $\alpha = 0.58$. Weight has a mean value of 70.488 lbf and a standard deviation of 8.45 lbf. Critics may label the robust design optimization calculations as academic because the range of variation is very small. The variation in the mean value of the weight was in the range 70.4863 to 70.4908 lbf. The range for standard deviation was 8.4499 to 8.4504 lbf. Robust design optimization is discussed further in Reference 2. Reliability-based optimization, also referred to as stochastic design optimization, is discussed next.

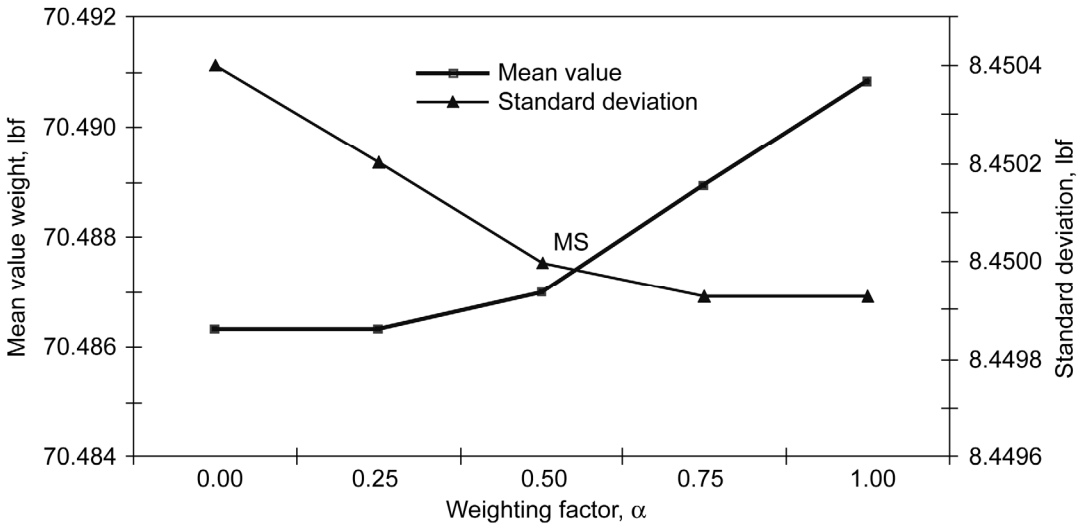

Figure 6.—Robust design optimization for three-bar truss.

Stochastic Design Optimization (SDO)

A stochastic optimization methodology has been developed to design components of an airframe structure that can be made of metallic and composite materials. The design is obtained as a function of the risk level, or reliability, *p*. The design method treats uncertainties in load, strength, and material properties as distribution functions, which are defined with mean values and standard deviations. A design constraint or a failure mode is specified as a function of *p*. Solution to stochastic optimization yields the weight of a structure as a function of *p*. Optimum weight versus *p* traced an inverted-S-shaped graph. The center of the S graph corresponds to 50 percent, $p = 0.5$, probability of success. A heavy design with weight approaching infinity can be produced for a near zero rate of failure that corresponds to unity for *p*, or $p = 1$. Weight can reduce to a small value for the most failure-prone design ($p = 0$). Reliability can be changed for different components of an airframe. For example, the landing gear can be designed for very high reliability, and reliability can be reduced to an extent for a raked wingtip. The SDO capability is obtained by combining three codes: (1) The MSC/Nastran code is the deterministic analysis tool, (2) the fast probabilistic integrator, or the FPI module of the NESSUS software, is the probabilistic calculator, and (3) NASA Glenn Research Center's optimization testbed CometBoards became the optimizer. The SDO capability requires four models: a finite element structural model, material model, load model, and design model. This paper illustrates the design capability by considering the example of a Boeing 767–400ER raked wingtip.

Formulation of Reliability-Based Design

The design testbed CometBoards has been extended into the stochastic domain. The objective is to determine the mean values of the design parameters that optimize the mean value of a merit function (such as weight), subject to a set of constraints. Variance in the weight can be back calculated. For stochastic optimization, the constraints g_j are derived from random response variables within prescribed random upper and lower bounds g_j^U and g_j^L, respectively, with a specified percent probability (*p* between 0 and 1), as: $P(g_j^L \le g_j \le g_j^U) \ge p$. A stochastic constraint (e.g., a stress limitation $\tau \le \tau_0$) can be expressed as

$$\overset{\text{Stochastic}}{g(p)} = \left[\left|\frac{\mu_{\tau_1}}{\mu_{\tau_{10}}}\right| - 1\right]^{\text{Mean value}} + \left[\varphi^*(p)\frac{\sqrt{\sigma_{\tau_1}^2 + \sigma_{\tau_{10}}^2}}{\mu_{\tau_{10}}}\right]^{\text{Standard deviation}} \leq 0 \tag{7}$$

where

p is the probability of occurrence

μ_{τ_1} is the mean value of stress

$\mu_{\tau_{10}}$ is the mean value of strength (stress allowable)

φ^* is the parameter phi critical

μ_{τ_1} is the standard deviation of stress

$\sigma_{\tau_{10}}$ is the standard deviation of stress allowable

The first term with superscript "Mean value" resembles a deterministic stress constraint. It is written in terms of the mean values of the response variable, here stress τ_1 has a mean value μ_{τ_1}. Strength or allowable stress τ_{10} has a mean value of $\mu_{\tau_{10}}$. The second term with superscript "Standard deviation" accounts for the standard deviations σ_{τ_1} and $\sigma_{\tau_{10}}$ in stress and strength τ_1 and τ_{10}, respectively. The inverse of the cumulative distribution function for the standard normal at probability level p is $\varphi^*(p)$. The stochastic constraint reduces to the familiar deterministic form, when the variation is set to zero.

$$\text{Lim}\begin{Bmatrix}\sigma_{\tau_1} \to 0 \\ \sigma_{\tau_{10}} \to 0 \\ \mu_{\tau_{10}} \to \text{allowable}\end{Bmatrix}\left[\left(\left|\frac{\mu_{\tau_1}}{\mu_{\tau_{10}}}\right| - 1\right) + \varphi^*(p)\frac{\sqrt{\sigma_{\tau_1}^2 + \sigma_{\tau_{10}}^2}}{\mu_{\tau_{10}}} \leq 0\right] = \overset{\text{Deterministic constraint}}{\left(\left|\frac{\mu_{\tau_1}}{\mu_{\tau_{10}}}\right| - 1\right)} \leq 0 \tag{8}$$

The derivation of the constraint expression in Equation (7) is straight forward. Consider a stress constraint ($|\tau| \leq \tau_0$) with a probability $\wp$ of occurrence of p:

$$\begin{aligned}\wp\left(|\tau| \leq \tau_0\right) &\geq p \\ \wp\left(|\tau| - \tau_0 \leq 0\right) &\geq p\end{aligned} \tag{9}$$

Considering the case when τ is greater than zero, the difference between the two random variables is set to a new random variable $\Re$:

$$\Re = \tau - \tau_0 \tag{10}$$

The new random variable is normalized to obtain a standard normal random variable Φ with mean 0 and variance 1:

$$\Phi = \frac{\Re - \mu_S}{\sigma_S} \tag{11}$$

Thus

$$
\begin{aligned}
&\wp\left(\Re \le 0\right) \ge p \\
&\wp\left(\Re - \mu_{\Re} \le 0 - \mu_{\Re}\right) \ge p \\
&\wp\left(\frac{\Re - \mu_{\Re}}{\sigma_{\Re}} \le \frac{0 - \mu_{\Re}}{\sigma_{\Re}}\right) \ge p \\
&\wp\left(\Phi \le -\frac{\mu_{\Re}}{\sigma_{\Re}}\right) \ge p
\end{aligned}
\tag{12}
$$

The probability $\wp\left(\Phi \le x\right)$ is the definition of the cumulative distribution function for the standard normal F_{Φ}. Thus

$$
F_{\Phi}\left(-\frac{\mu_{\Re}}{\sigma_{\Re}}\right) \ge p \tag{13}
$$

The minimum value of Φ at which the probability level, p, is satisfied is obtained from the inverse of the cumulative distribution function for the standard normal. This value is labeled "φ^*."

$$
\begin{aligned}
&\varphi^*\left(p\right) = F_{\Phi}^{-1}\left(p\right) \\
&\varphi^*\left(p\right) \le -\frac{\mu_{\Re}}{\sigma_{\Re}}
\end{aligned}
\tag{14}
$$

but

$$
\begin{aligned}
&\mu_{\Re} = \mu_{\tau} - \mu_{\tau_0} \\
&\sigma_{\Re}^2 = \sigma_{\tau}^2 + \sigma_{\tau_0}^2
\end{aligned}
\tag{15}
$$

So,

$$
\begin{aligned}
&\varphi^*\left(p\right) \le -\frac{\mu_{\tau} - \mu_{\tau_0}}{\sqrt{\sigma_{\tau}^2 + \sigma_{\tau_0}^2}} \\
&\varphi^*\left(p\right)\sqrt{\sigma_{\tau}^2 + \sigma_{\tau_0}^2} \le -\mu_{\tau} + \mu_{\tau_0} \\
&\mu_{\tau} - \mu_{\tau_0} + \varphi^*\left(p\right)\sqrt{\sigma_{\tau}^2 + \sigma_{\tau_0}^2} \le 0
\end{aligned}
\tag{16}
$$

Finally, taking the case $\tau < 0$, normalizing with respect to the mean of the allowable and combining gives

$$
\left[\left|\frac{\mu_{\tau}}{\mu_{\tau_0}}\right| - 1\right] + \left[\varphi^*\left(p\right)\frac{\sqrt{\sigma_{\tau}^2 + \sigma_{\tau_0}^2}}{\mu_{\tau_0}}\right] \le 0 \tag{17}
$$

or $g \le 0$

As mentioned earlier, the constraint has two parts. The first part is similar to a deterministic constraint specified in terms of the mean value of the variable. The second part contains the contribution from stochastic that included the inverse function and square of standard deviations as well as the mean value. For $p = 0.50$, φ^* is zero, and the constraint degenerates into a standard deterministic constraint. Observe that μ_τ is a response variable that is obtained from stochastic calculations and is not the same as the solution to the deterministic system.

In the above derivation, the two cases $\tau > 0$ and $\tau < 0$ were treated separately. In doing so, an assumption was made that $\mu_\tau \gg \sigma_\tau$. This is reasonable when the constraint is active. For $p = 0.25$, φ^* is –0.6745, and the constraint is relaxed. If it were an active constraint, the stochastic process becomes equivalent to increasing the allowable value. This would have a tendency to generate a lighter optimum design. For $p = 0.75$, φ^* is 0.6745, the constraint is tightened. If it were an active constraint, the stochastic process becomes equivalent to decreasing the allowable value. This would have a tendency to generate a heavier optimum design. The stochastic design will have a tendency to produce a lighter design when p is less than 50 percent, but a heavier design otherwise. The formulation of reliability-based design optimization is quite similar to that for the deterministic problem. The mean value of the design variable is generated to minimize the mean value of weight subjected to the stochastic constraints defined in Equation (7).

Numerical Examples for Reliability-Based Design Optimization

Reliability-based optimization is illustrated considering two components of an airframe structure. The first component is a web of an airframe stabilizer, and the second component is a racked wingtip. Examples are proprietary components of the Boeing Company and provided to us as a courtesy to advance reliability-based optimization concept for industrial applications. Sufficient information will be given to illustrate the concept.

Design Example 2: Web Plate of an Airframe Stabilizer

The inverted-S-shaped graph in reliability-based design optimization is illustrated considering the example of a web plate of an airframe stabilizer. The steel web plate, which was part of an aircraft stabilizer structure, was about 100 in. long, 12 in. wide, and 0.072 in. thick. It was idealized as a planar structure in the x,y-plane. The finite element model had CQUAD4 and CTRIA3 elements. Load was applied in the x,y-plane. Load was obtained by projecting the reactive load from the stabilizer into the plane of the web. The maximum von Mises stress for the initial design was 100 units psi with a maximum displacement of Δ milli-inch. Load, material properties, and design parameters were considered as random variables. The mean values were taken equal to their deterministic values with a 10-percent standard deviation. For example, the mean value of Young's modulus was 30 000 ksi, (which was its deterministic value) with a 10-percent standard deviation of 3000 ksi. The stochastic response calculation used three different probabilistic analysis methods. All three methods used MSC/Nastran for deterministic calculation. The FPI module was also used by all three methods. The methods used were

Method 1: This method used the first probabilistic integrator with normal distribution for all variables.

Method 2: A neural network and a regression method were trained for the three design variables. Normal distribution was used with the neural network approximation.

Method 3: This method replaced normal distribution with the Weibull function in method 2. The regression method was used for approximation.

There was little difference between the mean value and deterministic value for stress by all three methods. The standard deviation was about 9 percent, which compared well with the 10-percent deviation in the primitive random variables. The design model had three random variables, consisting of one thickness along the web boundary, one in the plate central zone, and one in between (the intermediate region). To begin optimization calculations, the mean value of the variables were taken equal to the deterministic optimum solutions. The standard deviations were 10 percent of the mean value for all three of the design variables. CometBoards testbed was used for design optimization. Optimum weights for different probability of failure are given in Table IV. The rate ranged from a vulnerable design (with 999 failures in 1000 samples) to a reliable design with 1 failure in 1000 samples.

Weight versus probability of success is plotted in Figure 7. There is some deviation in the weight calculated by the three different analysis methods as shown in the figure. For a 50-percent probability of success all three methods converged to 3.22 lbf for the optimum weight. For a reliable design with 1 failure in 1000 samples the first method produced about a 10-percent higher weight than that obtained by the neural network technique. The difference reduced to 5 percent for the regression method.

TABLE IV.—OPTIMUM WEIGHT VERSUS PROBABILITY LEVEL FOR WEB PLATE

(X) (X failures in 1000 samples)	Probability level, p	Optimum weight of web plate, lb		
		Method 1 FPI and normal distribution	Method 2 Neural network and normal distribution	Method 3 Regression method and Weibull function
(999)	0.001	1.16	1.78	1.75
(975)	0.025	1.89	2.26	2.22
(900)	0.1	2.33	2.56	2.54
(700)	0.3	2.84	2.94	2.93
(500)	0.5	3.22	3.22	3.22
(300)	0.7	3.61	3.52	3.52
(100)	0.9	4.21	3.99	3.98
(25)	0.975	4.81	4.47	4.41
(1)	0.999	5.96	5.40	5.16

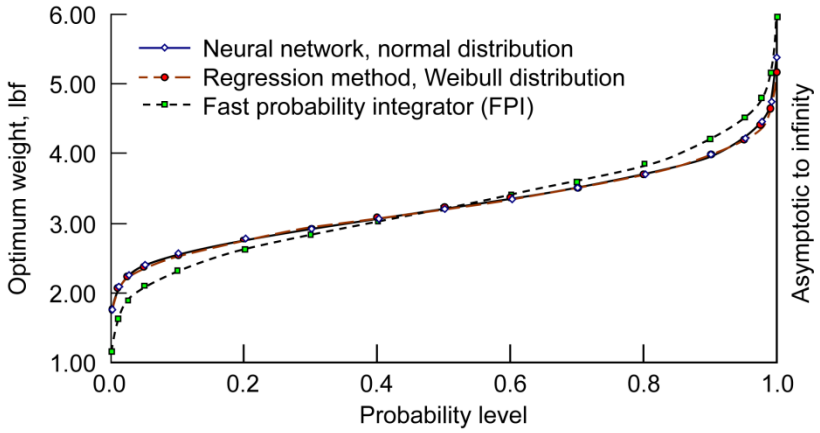

Figure 7.—Inverted-S graph for optimum weight versus probability level for web plate.

The Inverted-S-Shaped Graph

The weight versus probability of success for the web plate given in Table IV is plotted in Figure 7. Weight increased when reliability exceeded 50 percent. Weight decreased when the reliability was compromised. The weight versus reliability traced out the inverted-S-shaped graph. A design can be selected that depends on the level of risk acceptable to the situation. The inverted-S-shaped graphs were also generated for 20 examples given in Reference 2. The illustration in Figure 8 provides a simple explanation for the inverted-S shape of the graph.

Consider a deterministic design calculated for an allowable stress limit of 25 ksi with a 100 lbf weight for the structure (see Fig. 8(a)). The structure is redesigned next for a 50-percent probability of success. Assuming a 1.5 safety factor in applied loads, the stress can be approximated to 17 ksi and the proportioned weight can be approximated as 67 lbf (see Fig. 8(b)). Let us consider a reliable design with 1 failure in 100 000 samples. The stress value is likely to increase to 24 ksi because of an increase in the corresponding area under the distribution function (see Fig. 8(c)). The weight has to be increased to about 80 lbf because of a high value for stress, as shown in Figure 8(c). Consider next a failure-prone design with 90 failures in 100 samples. The stress can be less, like 7 ksi, because of a reduced area under the distribution function (see Fig. 8(d)). The weight can be reduced to about 28 lbf because of the low stress level. In reliability-based design optimization, weight can become very heavy when reliability approaches unity; likewise, a lightweight design can be obtained when reliability is compromised.

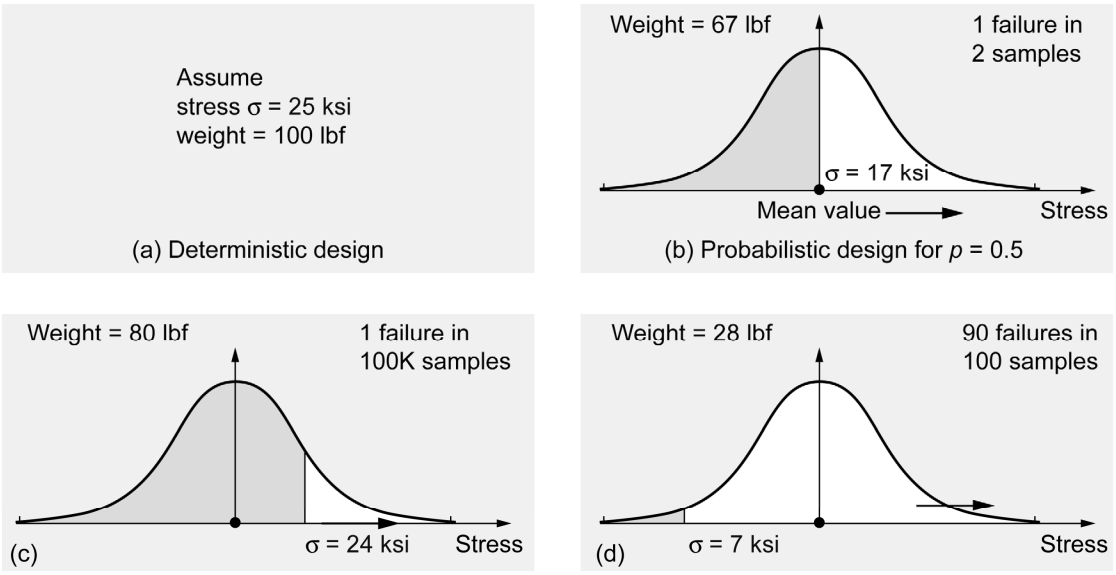

Figure 8.—Basic reliability design concept; a qualitative illustration for induced stress. (a) Deterministic design. (b) Design for mean value of reliability p = 0.5. (c) Design for more than mean value. (d) Design for less than mean value.

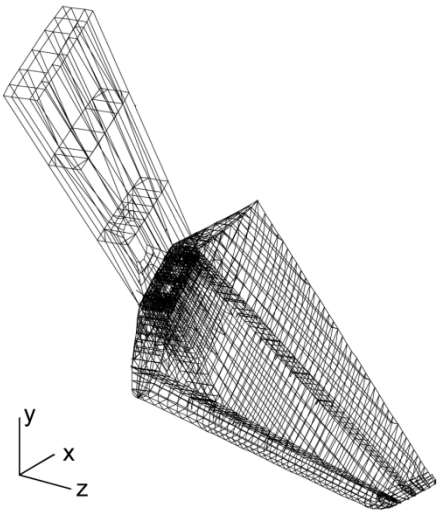

Figure 9.—Model of raked wingtip of Boeing 767–400 extended range airliner.

Design Example 3: Raked Wingtip Structure

Reliability-based optimization is illustrated considering the example of a composite airframe component of the Boeing 767–400 extended range airliner, the raked wingtip structure shown in Figure 9. The structure is fabricated out of component parts made of metallic and composite materials. The available industrial design is referred to as the initial design. It is required to generate a deterministic optimum design as well as a reliability-based design for the component. The problem is treated in five separate sections:

(1) Deterministic analysis
(2) Deterministic optimization
(3) Probabilistic analysis
(4) Probabilistic analysis for strain and displacement
(5) Reliability-based design optimization

Deterministic Analysis

The component has a wing-box type of construction with face sheets and web panels made of composite materials with an aluminum honeycomb core. Its components such as the root rib, tip rib, and leading edge parts are made of aluminum, and a set of titanium members are also used. The MSC/Nastran code was used as the deterministic analysis tool. The finite element model had about 3000 nodes and 17 000 degrees of freedom. The model was made of 3500 elements, consisting of CBAR, CBUSH, CELAS1, CHEXA, CONROD, CPENTA, CQUAD4, CROD, CSHEAR, and CTRIA3 elements. For aluminum, titanium, composite, and honeycomb materials, typical values were used for the material properties like Young's modulus, Poison's ratio, shear modulus, and others. The structure was subjected to eight load cases. The CPU time for a single MSC/Nastran run was about 5 s for static analysis, and it required almost 1 min to calculate a set of 20 frequencies on a Red Hat Enterprise Linux workstation, Release 4. Overall response of the initial model for the eight load cases is presented in Table V.

TABLE V.—NORMALIZED RESPONSE OF COMPOSITE RAKED WINGTIP
(MAXIMUM VALUE IS SET TO 100 UNITS)

Load case	Strain energy, *U*, in.-kip	Maximum displacement, in.	Maximum von Mises stress for metal, ksi	Maximum principal microstrain in composite laminates
1	17.22	–41.15	43.56	32.49
2	73.70	84.50	76.85	72.96
3	63.70	77.41	74.91	65.86
4	61.11	75.73	75.37	66.13
5	16.48	–40.50	40.48	34.81
6	100.00	100.00	100.00	100.00
7	82.04	91.01	96.69	93.44
8	52.22	77.49	70.24	55.96

The strain energy U in the first column in Table V was obtained as one-half of the product of load P and displacement X over all nodes using the following formula:

$$U = \left(\frac{1}{2}\right) \int_{\text{Volume}} (\text{strain} \times \text{stress})\, dv = \frac{1}{2}\left(\sum_{j=1}^{\text{All nodes and directions}} P_j X_j \right) \tag{18}$$

The strain energies for the eight load cases were in the range 16 to 100 normalized units. Load case 6 contained the peak value for strain energy of 100 units. The load case also contained the maximum displacement, maximum strain in the composite components, and maximum stress in metals. The structure was designed for the critical load case 6 and checked against other load cases. The concept to design for a load case with maximum strain energy drastically reduced the number of calculations in design optimization, and it was subsequently proved correct for the problem.

Deterministic Optimization

The objective of the optimization problem was to reduce the weight of the wingtip without changing its geometrical configuration. Only the thicknesses of the components were allowed to be adjusted within prescribed bounds. For design optimization the raked wingtip was separated into several substructures consisting of metallic and composite components. From a preliminary design optimization study it was concluded that the thickness of titanium components and aluminum parts like, root rib center section, leading and trailing edge webs, as well as leading edge and tip rib skins cannot be changed from a manufacturing consideration. Design variables associated with these parts were considered passive. The remaining four composite members were grouped to obtain a total of 13 active design variables. Grouping was on the basis of the number of laminates. For example, the first design variable represented a proportional thickness parameter for the upper and lower skin panels. The panel was made of laminates over a honeycomb core. This variable contained a total of 211 CQUAD4 and CTRIA3 elements. Likewise, the design variable 10 represented the area parameter for spars in the front web. The areas of the spars were grouped to obtain a design variable and 92 CROD elements were used in the discretization. Other design variables were defined in a similar manner.

For constraint formulation, the structure was separated into 203 groups of elements to obtain a total of 203 strain constraints for the upper and lower skin panels as well as the spars. The composite rod elements were grouped to obtain 16 more strain constraints. Three translations and one rotation were constrained at a tip node of the structure for load case 6 as well as for load case 7 to obtain eight displacement constraints. The design model has a total of 227 behavior constraints. Constraint can be imposed on principal strain, for a failure theory, or on a strain component. Displacement limitations along x-, y-, and z-directions were set at Δ_1, Δ_2, and Δ_3 in., respectively. Maximum rotation was not to exceed θ°. Design optimization was performed using the testbed CometBoards. Deterministic optimum solution

is given in Table VI. Only a normalized optimum solution can be given because of the proprietary nature of the data.

TABLE VI.—NORMALIZED DETERMINISTIC OPTIMUM SOLUTION

Design variable	Weight		
	Original design	Design model 1	Design model 2
	100 units[a]	84.0 units	80.0 units
		Change in percent (100 represents no change)	
1	100.0	70.1	70.1
2	100.0	104.5	99.83
3	100.0	110.3	111.83
4	100.0	75.64	76.97
5	100.0	44.85	44.45
6	100.0	123.35	80.96
7	100.0	84.17	94.45
8	100.0	44.08	44.88
9	100.0	86.12	83.59
10	100.0	88.09	88.09
11	100.0	73.83	73.83
12	100.0	100.00	100.00
13	100.0	100.00	100.00
Active strain constraints	100.0	6 active and 9 nearly active	6 active and 9 nearly active
Displacement in z-direction, in. (limit was Δ in.)	100.0	Nearly active	Nearly active
Rotation, deg (limit was θ°)	100.0	4.48	4.72
Frequency, Hz	100.0	16.45	20.33

[a]Normalized to 100 units.

Stress and strain obtained from the finite element model were presumed not to be accurate at some metal and composite interface locations. Such localized regions were avoided in design calculations by excluding the associated strain constraints. Table VI, column 2, model 1, refers to a configuration that was obtained by excluding the strain constraints for a set of interface elements. Likewise model 2 excluded strain constraints associated with another set of elements. Generation of an optimum solution for model 1, for example required about 39 CPU minutes. Optimum weight for model 1 was 16 percent lighter than that of the original design. The weight savings was 20 percent for model 2. Design changed throughout the structure except for variables 12 and 13, which represented the minimum thicknesses. Maximum reduction was observed for design variable 8 with a 44 percent change. The thickness reduced to 0.44 in. if the original value was 1 in. In other words, in the original structure the entire region that was associated with design variable 8 represented an overdesigned condition. The thickness variable 8 for model 1 increased to 124 percent from its assumed value of 100 percent, or the region originally was underdesigned. The design process redistributed the strain field with many active constraints. There was little change in the displacement state or frequency value for model 1. For model 2, maximum displacement reduced by 2.5 percent, but its frequency increased by 25 percent because of a 20 percent reduction in its weight.

Probabilistic Analysis

Probabilistic analysis requires a geometrical model, a load model, and a material model:

Geometrical model: All 13 design variables of the deterministic design optimization were considered to be random variables. Their mean values were equal to the deterministic optimum design solutions. Their standard deviations were set at 7.5 percent of the mean values. The thicknesses of the honeycomb were considered as random variables. Their mean values were equal to that of the initial design with a standard deviation of 10 percent of the mean values. Cross-sectional areas of the bars were considered to be deterministic parameters and were equal to the optimum solutions.

Load model: Each load component is considered to be a random variable with a mean value equal to 66.67 percent of the deterministic value, with a 10-percent standard deviation. For example, if a deterministic load component is 100 lbf, then its random counterpart would have 66.67 lbf for its mean value with 6.67 lbf for the standard deviation. Each load component was changed in a similar manner. This refers to load model A. A second load model was recommended and added. Thus, there were two load models, load model A and load model B. Load model B was generated following the procedure for load model A but with a reduced mean value of 0.50 percent of the deterministic load value. A standard deviation was set at 10 percent of the mean load value.

Material model: Modulus of elasticity as well as Poisson's ratio were considered to be random variables. The standard deviations for all the material parameters were set at 7.5 percent of their mean values. The mean values were set to 105 percent of their deterministic values for the Young's modulus and shear modulus of fabric as well as the shear modulus for the honeycomb. The mean value for Poisson's ratio was set to 100 percent of its deterministic value.

Probabilistic Solution for Strain and Displacement

The probabilistic solution was obtained using the MSC/Nastran code and the FPI module of the NESSUS software. Four different types of distributions were considered: normal distribution, Weibull function, lognormal, and Gumbel type 1 distributions. The probabilistic analysis produced the mean value of strain (in the element number 11531) to be 5050 microstrain by all four types of distribution functions (see row 1 in Table VII). Likewise, the standard deviation remained the same at 16 percent of the mean value by all four distribution functions. The mean value of displacement (at node 11243 in the z-direction) was 9.6 in. with a standard deviation of 10 percent by all four distributions. The observation that the mean values and standard deviations did not change for different distribution types was along the expected line.

TABLE VII.—PROBABILISTIC RESPONSE FOR DIFFERENT PROBABILITY LEVELS[a]

N samples	Microstrain in element 11531				Displacement at node 11243 along z-direction			
	Normal	Weibull	Lognormal	Gumbel type 1	Normal	Weibull	Lognormal	Gumbel type 1
Mean value	5050	5050	5050	5050	9.7	9.7	9.7	9.7
Standard deviation	810	810	810	810	0.98	0.98	0.98	0.98
2	5050	5123	4986	4917	9.7	9.7	9.6	9.4
1000	7555	6967	8162	9050	12.6	11.7	13.1	14.4
50 000	8379	7398	9599	11523	13.6	12.2	14.5	17.4
100 000	8507	7459	9843	11961	13.7	12.2	14.7	17.9
500 000	8903	7591	10402	12977	14.1	12.3	15.2	19.1
1 million	9264	7644	10641	13415	14.2	12.4	15.5	19.7
10 million	9264	7804	11424	14870	14.7	12.6	16.2	21.4

[a]The first and second rows provide the mean values and standard deviations. Remaining data represent mean values.

Probabilistic solution for the strain and the displacement for four different types of distributions for different failure rates is given in Table VII. For a 50-percent probability of failure, or one failure in two samples, the mean value and the calculated strain are equal at 5050 microstrain for normal distribution. The same is not true for Weibull, lognormal, or Gumbel type 1 distributions because of a lack of symmetry in such functions. Consider next, 1 failure in 1 million samples. The Weibull prediction was conservative. It was about 85 percent of the normal distribution for strain as well as displacement. Estimates by Gumbel type 1 distribution was on the higher side. For 1 failure in 1 million samples, it predicted about 40 to 45 percent higher strain and displacement than that for the normal distribution function.

Reliability-Based Design Optimization

Probabilistic optimization is performed for the two deterministic design models, models 1 and 2, as discussed earlier (see Table VI). The probabilistic design calculation used the information given for stochastic analysis along with additional data required to formulate failure modes or the design constraints. It was assumed that mean value of allowable strain was 25 percent higher than its deterministic limit, while the standard deviation was set at 7.5 percent of the mean value. For example, the limits for strain were set with a mean value of ε microstrain and a standard deviation of ε/10. From deterministic optimization calculations, it was observed that only the displacement limitation along the z-direction and rotation had some influence in the design while other stiffness constraints were quite passive. Thus, for probabilistic design only two stiffness constraints were retained. At node 11243, along the z-direction, the mean value and standard deviation for the displacement limit were 1.25Δ and 0.125Δ in., respectively. The mean value and standard deviation for rotation limit were set at 1.25θ and 0.125θ, respectively. For the design calculation normal distributions were assumed for all random parameters.

The optimization calculation required continuous running of the code for more than 5 days, but the execution was smooth and eventless. The stochastic optimum solution was quite similar to that obtained for deterministic optimization depicted in Table VI. There were numerous active strain, displacement, and rotation constraints. Normalized optimum weight obtained for different failure rates is given in Table VIII.

TABLE VIII.—PROBABILITY OF FAILURE VERSUS WEIGHT

Samples, *N*	Normalized optimum weight			
	Design model 1 and load case A (strength + stiffness)	Design model 1 and load case A (strength only)	Design model 1 and load case B [strength or (strength + stiffness)]	Design model 2 and load case A (strength + stiffness)
2	64.68	64.68	62.24	63.20
10	67.43	67.43	63.57	64.36
100	70.47	70.47	65.51	66.97
1000	73.75	73.75	66.97	69.57
10 000	76.64	76.64	68.23	72.48
100 000	79.28	79.03	69.70	76.25
1 000 000	92.93	82.27	71.57	91.21
1 250 000	94.88	82.55	71.76	93.41
2 000 000	100.00	83.15	72.16	98.60

The normalized optimum weight was set to 100 units for strength and stiffness constraints for load case A in design model 1 for 1 failure in 2 million samples. This design exhibited nine active constraints consisting of eight strain and one displacement limitation. For an active stochastic constraint the first factor in Equation (7) (based on mean values) was equal to the second factor (which was a function of standard deviation and the phi critical parameter) in magnitude but with opposite sign. The frequency was 15.94 Hz for the optimum solution. One SDO run with 61 *p* levels required 128 h, or 5.33 days.

The Inverted-S-Shaped Graph

The weight versus probability of success given in Table VIII is plotted in Figures 10 and 11. In Figure 10, the x-axis represents N (as in one failure in N samples) and it begins at $N = 2$, or 50 percent probability of success. This graph represents one-half of the inverted-S graph because probability less than 50 percent is not included. This graph is for load case A, design model 1; both strength and stiffness constraints are considered, and column 1 in Table VIII contains the weight information.

The same information is replotted in Figure 11, but a logarithmic scale, or log(N), is used along the x-axis. This figure can be approximated into two linear segments. At the intersection point (SD) both strength and stiffness constraints are active. From the origin to the point SD, only strength constraints are active. From point SD onwards, both strain and stiffness constraints are active.

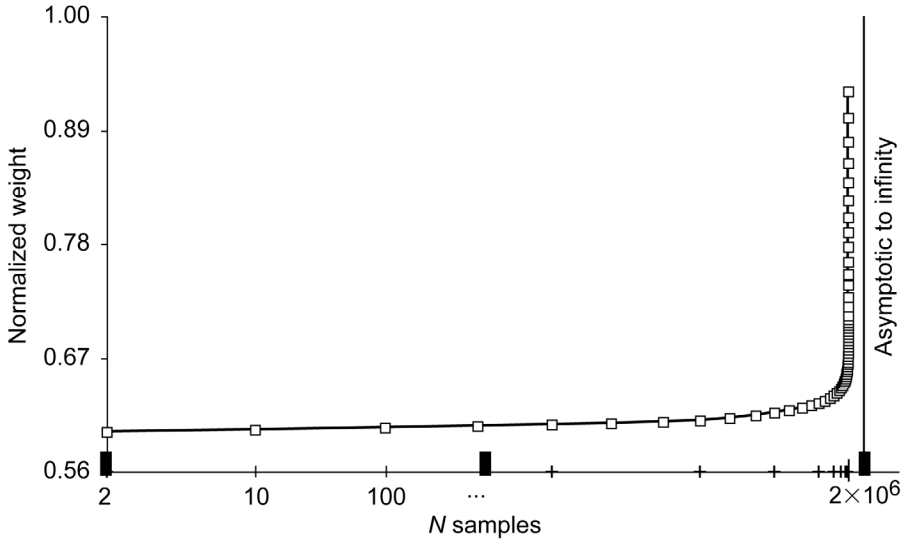

Figure 10.—Half of inverted-S graph for design model 1 and load case A.

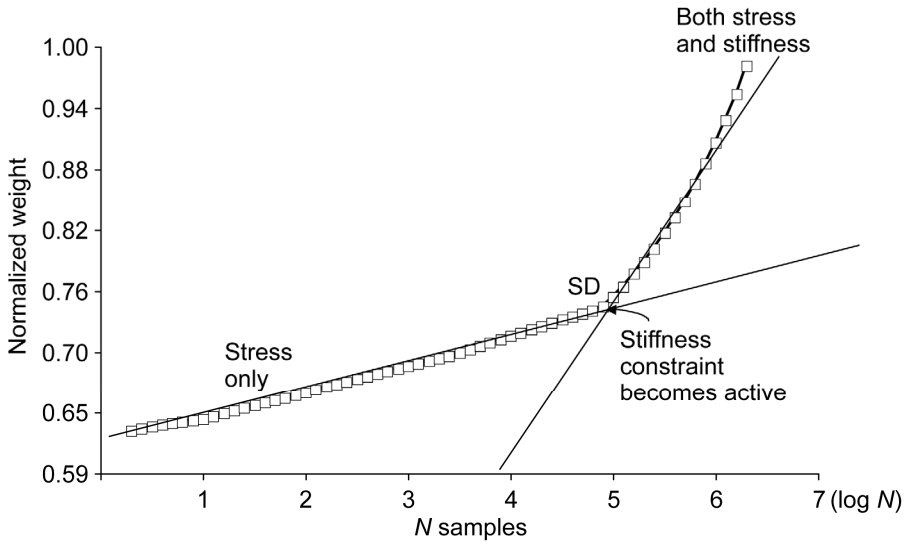

Figure 11.—Inverted-S graph in log scale for design model 1 and load case A.

The variation of weight shown in Table VIII was as expected. The weight is least for a 50-percent rate of success, or for $N = 2$. The weight increased when failure rate was reduced. The weight in the first two columns in Table VIII coincided up to 1 failure in 10 000 samples because only strength constraints were active. The weight increased when both strength and stiffness constraints became active (see column 2, in Table VIII). Weight shown in column 4 was lighter than that in column 2 because load model B was less severe than load model A. Weight shown in column 5 was lighter than that in column 2 because design model 2 was obtained by removing few severe strain constraints from model 1.

The distribution of the strain state in the wingtip is illustrated in Figure 12 for three cases. The first case is the initial design that was obtained by the industry. The second one is the deterministic solution while the third one represents the stochastic design. The strain distribution is uneven for the initial design, and strain exceeds 4000 microstrain at a few localized locations. The distribution of the strain state is more even for the deterministic as well as the stochastic design solutions.

Optimum weight for six design cases are depicted in Figure 13 in a bar chart. The first case with a weight assumed at 100 units represents the original design. All five calculated design cases have lower weight than the original design. The deterministic optimum solution (for strength and stiffness constraints with design model 1 and load case A) generated a 15.5-percent lighter design than the original design. The weight decreased further to 80.9 units when the stiffness constraint was relaxed (see design case 3). Stochastic optimization produced a mean value for the weight of 83 units with a standard deviation of 1.3 units for strength constraints for design model 1 and load case A for 1 failure in 1 million samples (see design case 4). The mean value for the weight and a standard deviation increased to 94 and 1.26 units when stiffness constraint was added to strength limitation (see design case 5). The mean value of weight and standard deviation reduced to 91.7 and 1.23 units, respectively, for strength and stiffness constraints for design model 2 and load case B (see design case 6 in Fig. 13). Overall, weight can be reduced up to 20 percent depending on the choice for model for design, load, and rate of failure. The standard deviation was small and remained at about 1 percent for the three design cases 4 to 6.

Sensitivity analysis was performed for the principal strain (in element 11531) for deterministic as well as SDO methods and are depicted in Figure 14. The element strain was most sensitive to load and elastic modulus E for fabric as well as for design variable 6 (DV6, see Table VI) that contained element 11531. The other 19 random variables were not sensitive to the strain. Both deterministic as well as stochastic methods identified the same set of variables, namely DV6, load, and Young's modulus.

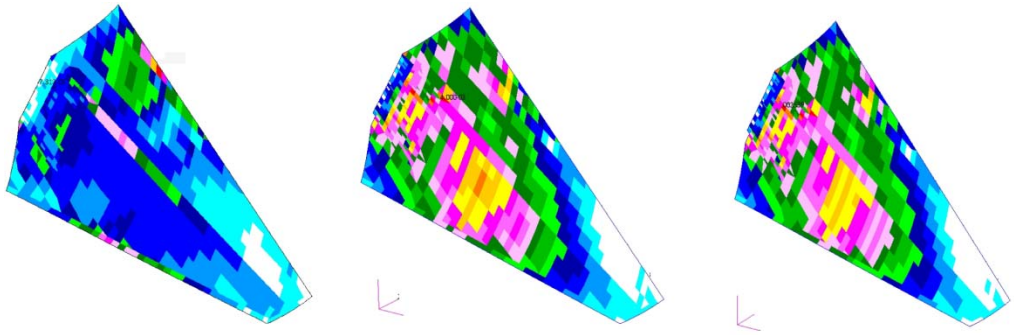

Figure 12.—Optimization process more evenly distributed the strain field in wingtip.

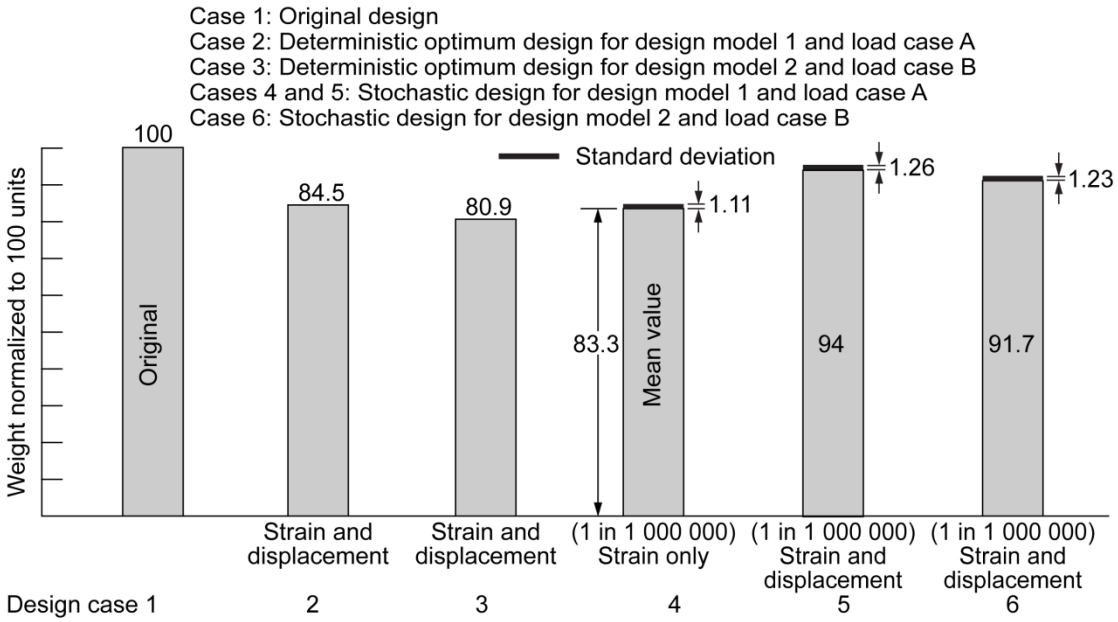

Figure 13.—Optimum weight for six design cases.

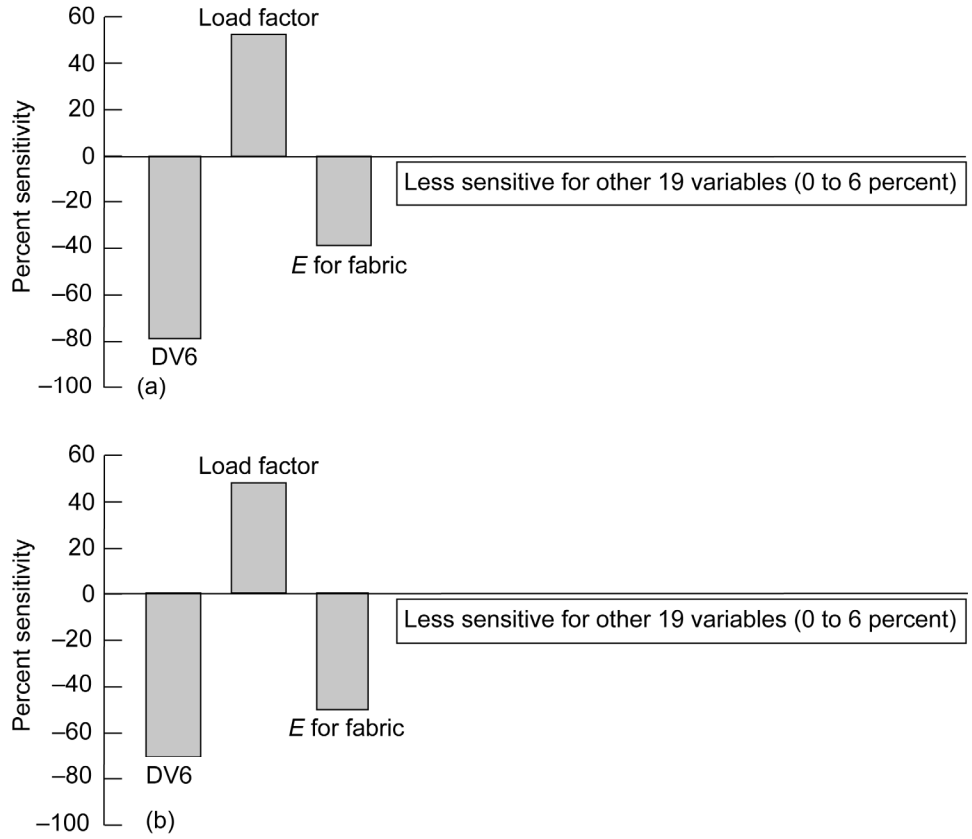

Figure 14.—Sensitivity analysis for principal strain in element 11531, where DV6 refers to design variable 6 and *E* is elastic modulus. (a) Deterministic design optimization. (b) Stochastic design optimization.

The CPU time to solution is given in Table IX. The calculation used CometBoards, which is NASA in-house software, along with MSC/Nastran version 2005.5.0 (2005R3), and the FPI module of NESSUS level 6.2 code (1995). Calculations used a Red Hat Linux 2.6.9-67.ELsmp O/S, with x86_64 architecture, 2600 MHz, 4 cpu, 8 GB of memory, and 32-bit numeric format.

One static analysis cycle required about 5 CPU seconds. The run time increased to 51 s for dynamic analysis. Stochastic analysis required about 47 min. Deterministic optimization required about 39 min. The CPU time for stochastic optimization was enormous at 126 to 128 h of continuous calculations.

TABLE IX.—CPU TIME FOR DESIGN AND ANALYSIS OF WINGTIP[a]

Activity	CPU time
One static analysis cycle in MSC/Nastran	5 s
Dynamic analysis to calculate 20 frequencies in MSC/Nastran	51 s
Deterministic optimization for design model 1	39 min
Stochastic analysis	47 min
Stochastic optimization: design model 1 and load case A	128 h
Stochastic optimization: design model 2 and load case A	126 h

[a]CPU is central processing unit.

Conclusions

The testbed CometBoards with MSC/Nastran and a Fast Probability Integrator successfully generated reliability-based design optimization for an industrial strength raked wingtip structure of a Boeing 767–400 extended range airliner made of metallic and composite materials. The optimization run required 128 h of execution.

The optimization methodology requires probabilistic models for load, material properties, failure theory, and design parameters. Accuracy of the design solution depends on the models.

Stochastic optimum weight versus reliability traced out an inverted-S-shaped graph. Weight increased when risk was reduced and vice versa. The inverted-S graph degenerated into linear segments when a logarithmic scale was used for the x-axis.

The optimization process redistributed the strain field in the structure and achieved up to a 20-percent reduction in weight over traditional design. Optimum weight was comparable between a deterministic solution and a highly reliable stochastic design. Inclusion of standard deviation as an additional objective function should be examined further because it offers very little variation and has insignificant impact. It may be a manufacturing issue with little relevance to analytical design calculations.

Design of an aircraft structural component has to be obtained for multiple load conditions. The maximum strain energy criteria identified a few critical load cases from the many load conditions. The design generated for the critical load was satisfactory. This approach reduced calculations to a very great extent.

The design sensitivity can identify critical zones for redesign consideration. Both deterministic and stochastic concepts identified identical zones. There was no preference to either concept.

References

1. Guptill, J.D., et al.: Extension of Optimization Test Bed CometBoards to Probabilistic Design. 6th Annual FAA/Air Force/NASA/Navy Workshop on the Application of Probabilistic Methods to Gas Turbine Engines, Solomons Island, MD, 2003.
2. Wei, X.: Stochastic Analysis and Optimization of Structures. Ph.D. Dissertation, Univ. of Akron, Akron, OH, 2006.
3. Thacker, B.H., et al.: Probabilistic Engineering Analysis Using the NESSUS Software. Struct. Saf., vol. 28, nos. 1–2, 2006, pp. 83–107.
4. Guptill, J.D., et al.: CometBoards User Manual Release 1.0. NASA TM–4537, 1996.
5. Cochran, W.G.: Sampling Techniques. John Wiley, New York, NY, 1977.

6. Kleiber, M.; and Hien, T.D.: The Stochastic Finite Element Method, John Wiley & Sons, New York, NY, 1992.
7. Cambou, B.: Application of First-Order Uncertainty Analysis in the Finite Element Method in Linear Elasticity. Proceedings of the 2nd International Conference Appl. of Statistics and Probability in Soil and Struct. Engrg., London, England, 1975, pp. 67–87.
8. Cornell, C.A.: First Order Uncertainty Analysis in Soils Deformation and Stability. Proceedings of the 1st Conf. Appl. of Statistics and Probability in Soil and Struct. Engrg., 1971, pp. 129–144.
9. Hisada, T.; and Nakagori, S.: Stochastic Finite Element Method Developed for Structural Safety and Reliability. Proceedings of the 3rd International Conference Struct. Safety Reliability, Trondheim, Norway, 1981, pp. 409–417.
10. Handa, K.; and Anderson, K.: Application of Finite Element Methods in Structural Safety and Reliability. Proceedings of the 4th International Conference on Structural Safety and Reliability, Kobe, Japan, 1981, pp. 385–394.
11. Benaroya, H.; and Rehak, M.: Finite Element Methods in Probabilistic Structural Analysis: A Selective Review. App. Mech. Rev., vol. 41, no. 5, 1988.
12. Elishakoff, I.; and Ren, Y.J.: Some Critical Observations and Attendant New Results in the Finite Element Method for Stochastic Problems. Chaos, Solutions & Fractals, vol. 7, no. 4, 1996, pp. 597–609.
13. Schuëller, G.I.: Computational Stochastic Mechanics—Recent Advances. Comput. Struct., vol. 79, 2001, pp. 2225–2234.
14. Patnaik, S.N.; Berke, L.; and Gallagher, R.H.: Integrated Force Method Versus Displacement Method for Finite Element Analysis. Int. Jnl. Computers Structures, vol. 38, 1991, pp. 377–407.
15. Patnaik, S.N., et al.: Improved Accuracy for Finite Element Structural Analysis Via an Integrated Force Method. Int. Jnl. Computers Structures, vol. 46, 1992, pp. 521–542.
16. Macsyma, Mathematics and System Reference Manual. Fifteenth ed., Macsyma, Inc., 1995.
17. ANSYS Release 9.0 Documentation. ANSYS, Inc., SAS IP Inc., 2004.
18. Shinozuka, M.: Monte Carlo Simulation of Structural Dynamics. Int. Jnl. Computers Structures, vol. 2, 1972, pp. 855–874.

REPORT DOCUMENTATION PAGE		Form Approved OMB No. 0704-0188

The public reporting burden for this collection of information is estimated to average 1 hour per response, including the time for reviewing instructions, searching existing data sources, gathering and maintaining the data needed, and completing and reviewing the collection of information. Send comments regarding this burden estimate or any other aspect of this collection of information, including suggestions for reducing this burden, to Department of Defense, Washington Headquarters Services, Directorate for Information Operations and Reports (0704-0188), 1215 Jefferson Davis Highway, Suite 1204, Arlington, VA 22202-4302. Respondents should be aware that notwithstanding any other provision of law, no person shall be subject to any penalty for failing to comply with a collection of information if it does not display a currently valid OMB control number.
PLEASE DO NOT RETURN YOUR FORM TO THE ABOVE ADDRESS.

1. REPORT DATE *(DD-MM-YYYY)*	2. REPORT TYPE	3. DATES COVERED *(From - To)*
01-04-2009	Technical Memorandum	

4. TITLE AND SUBTITLE
Reliability-Based Design Optimization of a Composite Airframe Component

5a. CONTRACT NUMBER

5b. GRANT NUMBER

5c. PROGRAM ELEMENT NUMBER

6. AUTHOR(S)
Patnaik, Surya, N.; Pai, Shantaram, S.; Coroneos, Rula, M.

5d. PROJECT NUMBER

5e. TASK NUMBER

5f. WORK UNIT NUMBER
WBS 6598.77.02.03.0531.02

7. PERFORMING ORGANIZATION NAME(S) AND ADDRESS(ES)
National Aeronautics and Space Administration
John H. Glenn Research Center at Lewis Field
Cleveland, Ohio 44135-3191

8. PERFORMING ORGANIZATION REPORT NUMBER
E-16553-1

9. SPONSORING/MONITORING AGENCY NAME(S) AND ADDRESS(ES)
National Aeronautics and Space Administration
Washington, DC 20546-0001

10. SPONSORING/MONITORS ACRONYM(S)
NASA; AIAA

11. SPONSORING/MONITORING REPORT NUMBER
NASA/TM-2009-215501; AIAA-2008-5879

12. DISTRIBUTION/AVAILABILITY STATEMENT
Unclassified-Unlimited
Subject Category: 39
Available electronically at http://gltrs.grc.nasa.gov
This publication is available from the NASA Center for AeroSpace Information, 301-621-0390

13. SUPPLEMENTARY NOTES

14. ABSTRACT
A stochastic design optimization methodology (SDO) has been developed to design components of an airframe structure that can be made of metallic and composite materials. The design is obtained as a function of the risk level, or reliability, *p*. The design method treats uncertainties in load, strength, and material properties as distribution functions, which are defined with mean values and standard deviations. A design constraint or a failure mode is specified as a function of reliability *p*. Solution to stochastic optimization yields the weight of a structure as a function of reliability *p*. Optimum weight versus reliability *p* traced out an inverted-S-shaped graph. The center of the inverted-S graph corresponded to 50 percent ($p = 0.5$) probability of success. A heavy design with weight approaching infinity could be produced for a near-zero rate of failure that corresponds to unity for reliability *p* (or $p = 1$). Weight can be reduced to a small value for the most failure-prone design with a reliability that approaches zero ($p = 0$). Reliability can be changed for different components of an airframe structure. For example, the landing gear can be designed for a very high reliability, whereas it can be reduced to a small extent for a raked wingtip. The SDO capability is obtained by combining three codes: (1) The MSC/Nastran code was the deterministic analysis tool, (2) The fast probabilistic integrator, or the FPI module of the NESSUS software, was the probabilistic calculator, and (3) NASA Glenn Research Center's optimization testbed CometBoards became the optimizer. The SDO capability requires a finite element structural model, a material model, a load model, and a design model. The stochastic optimization concept is illustrated considering an academic example and a real-life raked wingtip structure of the Boeing 767-400 extended range airliner made of metallic and composite materials.

15. SUBJECT TERMS
Deterministic; Stochastic; Risk; Industrial problem; CometBoards; Distribution; Normal; Weibull; Strain energy; Inverted S-graph

16. SECURITY CLASSIFICATION OF:			17. LIMITATION OF ABSTRACT	18. NUMBER OF PAGES	19a. NAME OF RESPONSIBLE PERSON
a. REPORT	b. ABSTRACT	c. THIS PAGE			STI Help Desk (email:help@sti.nasa.gov)
U	U	U	UU	34	19b. TELEPHONE NUMBER *(include area code)* 301-621-0390